Two-Dimensional Ni-BPDC MOF nanosheets supported low-Pt catalyst for high-performance hydrogen evolution

Xuliang Zhang[a,b], Haozhe Shen[a], Wen Zhang[c], Shuang Ma[a,b*], Gang Tian[a], Jiangwei Zhao[a], Tolkyn S. Baizhumanova[d], Svetlana A. Tungatarova[d], Xiangqian Li[a*], Heng Zhang[a*]

[a]School of Chemical & Environmental Engineering (Key Lab of Ecological Restoration in Hilly Areas), Pingdingshan University, Pingdingshan, Henan 467000, P.R. China

[b]Henan Province Engineering Technology Research Center of Green Hydrogen & Electrochemical Energy Storage

[c]College of Animal Science and Technology, Shandong Agricultural University, Tai'an, Shandong 271017, P.R. China

[d]al-Farabi Kazakh National University, 71, al-Farabi str., Almaty, 050040, Kazakhstan

1. Experimental Section

1.1 Materials and reagent

Nickel (II) nitrate hexahydrate ($Ni(NO_3)_2 \cdot 6H_2O$), Diphenyldicarboxylic acid (BPDC), N,N-Dimethylformamide (DMF) and ethanol were purchased from Aladdin Industrial Corporation. $PtCl_2$ was purchased from Acmec. 5% Nafion solution, Platinum powder (Pt/C, 20wt%) was provided by Sigma Aldrich Corporation. Ni Foam with a thickness of 1.6 mm and 120 ppi (pore per square inch) was purchased from Jia Shide Foam Metal Co., Ltd (Suzhou, China). All chemical reagents were used without any further purification.

1.1.1 Preparation of Ni-BPDC

The Ni-BPDC was synthesized by a typical solvothermal procedure. Firstly, the 1 cm × 2 cm nickel foam (NF) underwent multiple rounds of washing with 3 M hydrochloric acid, ethanol, and ultrapure water. Then, 0.3 mmol of $Ni(NO_3)_2 \cdot 6H_2O$ and 80 mg of 4,4'-Biphenyldicarboxylic acid were first dissolved in a mixed solvent of 12 mL DMF and 1 mL deionized water. Subsequently, the obtained solution and NF was transferred into 25 mL of Teflon-lined autoclave and heated at 130 ºC for 12 h. After cooling to room temperature, Ni-BPDC was obtained in situ on NF, and the sample was repeatedly washed with anhydrous ethanol. Finally, dry in a vacuum oven at 60 °C. For comparison, nano block Ni-BPDC containing different Ir loads were synthesized by changing the content of IrCl3 (1 and 5mg), respectively.

1.1.2 Preparation of bulk Ni-BPDC

For comparison, bulk Ni-BPDC was synthesized by a controlled temperature program. The temperature was increased stepwise at a rate of 10 °C per 60 min until reaching 120 °C, and then maintained at 120 °C for 72 h. Subsequently, the reaction system was cooled to room temperature at a rate of 10 °C per 10 h. The obtained product was collected by centrifugation, washed with ethanol, and dried under vacuum.

1.1.3 Preparation of Pt/Ni-BPDC

Disperse 2 mg of $PtCl_2$ in 15 mL of anhydrous ethanol and stir vigorously. The

solution and Ni-BPDC grown on NF were then transferred to a 25 mL Teflon-lined autoclave and heated at 100 °C for 10 hours. After cooling down to room temperature, washed with absolute ethanol, and then dried under vacuum at 60 °C overnight.

1.2 Materials characterization

The morphology and structure of the synthesized MOF are characterized by field emission scanning electron microscopy (FESEM, JSM-6700F) at an acceleration voltage of 15 kV. Transmission electron microscopy (TEM), and energy dispersive X-ray spectroscopy (EDS) images were recorded on a Talos F200X at an acceleration voltage of 300 kV. The X-ray diffraction (XRD) patterns of the samples were acquired by using a Bruker D8 Advance powder diffractometer with Cu Kα radiation (λ = 1.5418 Å) at a scan rate of 5° min^{-1} in the 2 theta range of 5°~60°. High resolution elemental analyses of Ni-BPDC and Ir@Ni-MOF samples loaded on nickel foam were carried out using an ESCALAB 250ix X-ray photoelectron spectrometer (XPS) with Al-Kα radiation, respectively. The collected XPS spectra was calibrated by referencing the binding energy of C 1s to 284.60 eV. The Pt content in Pt/@-BPDC was determined by inductively coupled plasma mass spectrometry (ICP-MS, Themo Fisher Scientific). (The sample powder was scraped from the nickel foam and dissolved by wet digestion with a mixture of concentrated sulfuric acid and nitric acid.)

1.3 Electrochemical measurements

Electrochemical measurements were performed with a workstation (CHI 660E, Shanghai, China) in a typical three-electrode configuration consisting of a platinum wire (the counter electrode), Hg/HgO (the reference electrode) and the active material (the working electrode) in 1.0 M KOH solution. The loads of Ni-BPDC and Pt/Ni-BPDC are 1.354 and 1.271 mg cm^{-2}, respectively. The measured potentials were given according to the following formula: E(RHE) = E(Hg/HgO) + 0.059 × pH + 0.098. Linear sweep voltammetry (LSV) and cyclic voltammetry (CV) measurements were performed to evaluate the HER properties of catalysis. For comparison, a benchmark Pt/C catalyst on Ni foam was fabricated by the following steps: 784 μL ethanol, 20 μL Nafion, 196 μL deionized water and 5 mg Pt/C were mixed to prepare dispersion and sonicated for 30 minutes. Finally, a certain of prepared dispersion was add on the NF.

The linear sweep voltammetry (LSV) curves were recorded with a scan rate of 5 mV s^{-1}. The Tafel slope was calculated by fitting the linear portion of the Tafel plots, obtained by using the Tafel equation [$\eta = b \log(j) + a$]. And all the polarization curves were corrected by the iR-drop compensation. The electrochemical impedance spectroscopy (EIS) was performed to cover the frequency interval from 0.01 Hz to 100 kHz with a 10 mV amplitude.

Electrochemical capacitance measurements were used to determine the active surface area of each catalyst. To estimate the electrochemical active surface area of the electrocatalysts, double-layer capacitance (C_{dl}) was considered in the non-faradaic region (-0.8 ~ -0.9 V vs. Hg/HgO) of CVs recorded at different scan rates of 20, 40, 60, 80,100 and 120 mV s^{-1}. Finally, the ECSA was obtained through dividing C_{dl} by the specific capacitance of electrode material. Generally, the specific capacitance for flat surface electrodes is 0.04 mF cm^{-2}.

1.4 Mass Activity calculated

Mass Activity (MA) = Catalytic Activity (CA) / Mass of Catalyst (MC)

where catalytic activity is the rate of the target reaction (e.g., current density, reaction rate) obtained from the experimental data and mass of catalyst is the total mass of the Pt@Ni-BPDC.

1.5 Turnover frequency calculations

The TOF (s^{-1}) values were calculated with the following equation: TOF = I/mnF

I: Current (A) during the linear sweep voltammetry (LSV) tests in 1 M KOH.

n: Number of active sites (mol).

F: Faraday constant (C mol^{-1})

m: The factor 1/m represents that m electrons are required to form one H_2 molecule from water, which means that the m values for hydrogen evolution and oxygen evolution reactions are 2. in 1 M KOH solution, we can get the corresponding TOF values to be 0.799 and 0.036 H_2/s per surface site of Pt/Ni-BPDC and Ni-BPDC.

1.6 ECSA calculation

Electrochemical capacitance measurements were used to determine the active surface area of each catalyst. To estimate the electrochemical active surface area of the electrocatalysts, double-layer capacitance (C_{dl}) was considered in the non-faradaic region (-0.654 ~ -0.714 V vs. RHE) of CVs recorded at different scan rates of 20, 40, 60, 80, 120 and 140 mV s-1. Then, plotting the double-layer charging current at -0.684 V vs. scan rate yields a linear slope, which is equivalent to twice the value of Cdl. Finally, the ECSA was obtained through dividing Cdl by the specific capacitance of electrode material. Generally, the specific capacitance for flat surface electrodes is 0.06 mF cm-2.

1.5 DFT Computational method

All spin-polarized density functional theory calculations were performed using the Vienna ab initio simulation package (VASP).[1] We employed the projector augmented wave (PAW) method[2] and pseudopotentials to describe ion-electron interactions, and used the Perdew-Burke-Ernzerhof (PBE)[2] generalized gradient approximation (GGA)[3] to describe electron-electron interactions. Van der Waals interactions were treated using the DFT-D3 method.[4] The initial structures were obtained from the Materials Project.[5] To investigate surface reactions, slab models with a vacuum region of 15 Å were constructed, with bottom atoms fixed at bulk positions. During optimization, the plane wave cutoff energy was set to 450 eV, energy convergence criteria were set to $1e^{-5}$ eV, and force convergence criteria were set to 0.03 eV $Å^{-1}$.

1.J. Hafner, Ab-initio simulations of materials using VASP: Density-functional theory and beyond, J. Comput. Chem. 29 (2008), 2044-2078.

2.P. E. Blöchl, Projector augmented-wave method, Phys. Rev. B. 50 (1994), 17953.

3.J. P. Perdew, K. Burke, M. Ernzerhof, Generalized gradient approximation made simple, Phys. Rev. Lett. 77 (1996), 38653868.

4.S. Grimme, S. Ehrlich, L. Goerigk, Effect of the damping function in dispersion corrected density functional theory, J. Comput. Chem. 32 (2011), 1456-1465

Figure

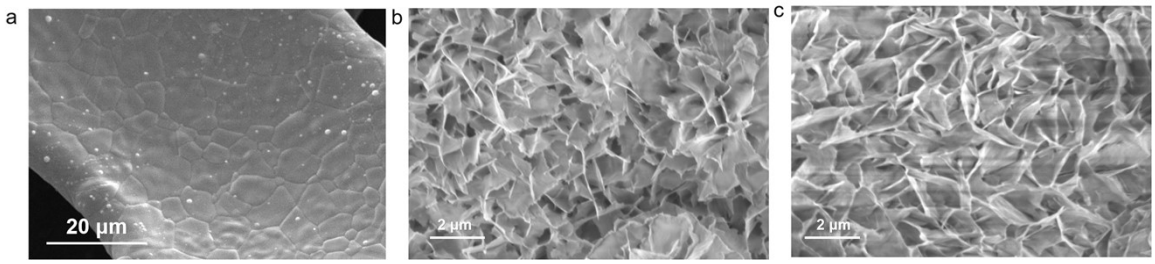

Fig. S1. SEM image of (a) bare NF (b) Ni-BPDC and (c) Pt/Ni-BPDC.

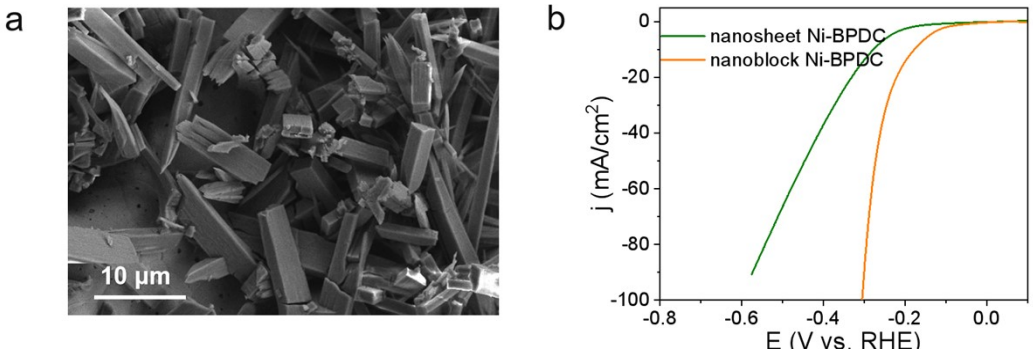

Fig. S2. (a) SEM image of nanoblock Ni-BPDC. (b) LSV curve of nanoblock Ni-BPDC and nanosheet Ni-BPDC.

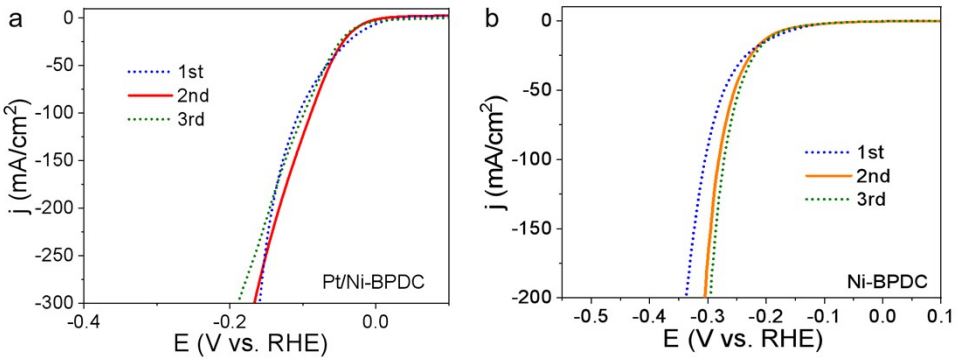

Fig. S3. The median value after three LSV tests.

To confirm the reproducibility of the electrocatalytic performance, three independent electrodes prepared under the same conditions were tested. The polarization curves (Fig. S3) show excellent consistency, further supporting the reliability of the Pt loading value.

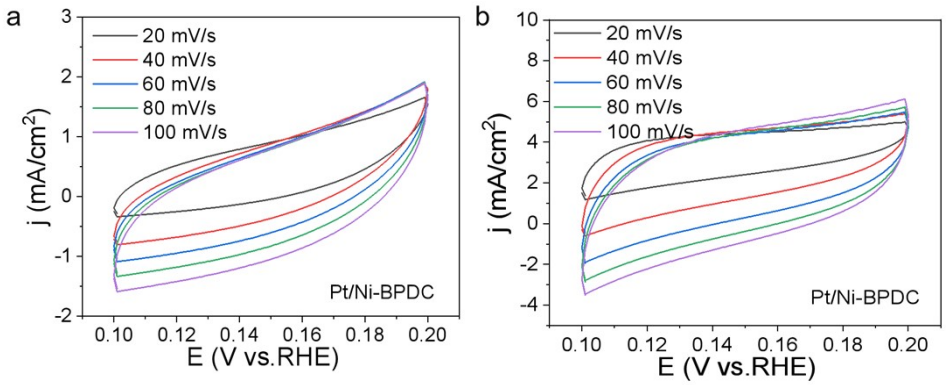

Fig. S4. CV curves at different scan rates for (a) Ni-BPDC and (b) Pt/Ni-BPDC.

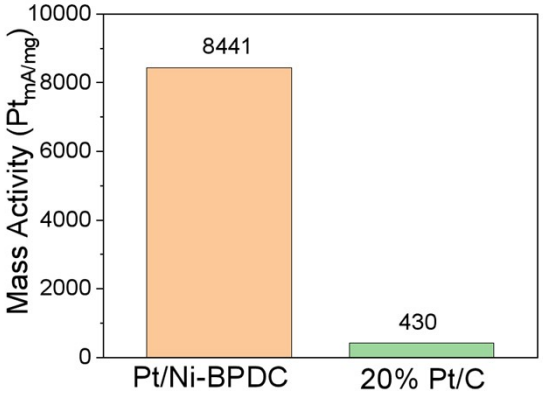

Fig. S5. Mass activity of Pt/Ni-BPDC and 20% Pt/C.

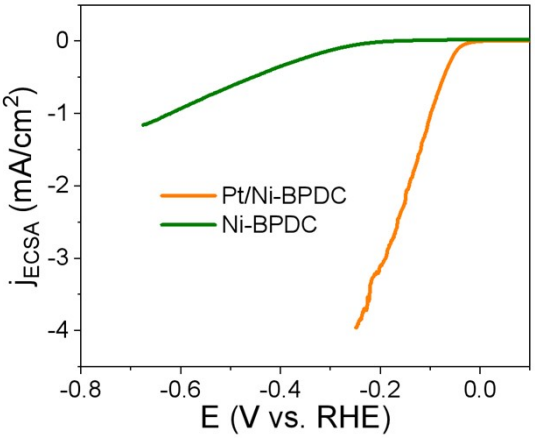

Fig. S6. ECSA-normalized polarization curves of Pt/Ni-BPDC and Ni-BPDC.

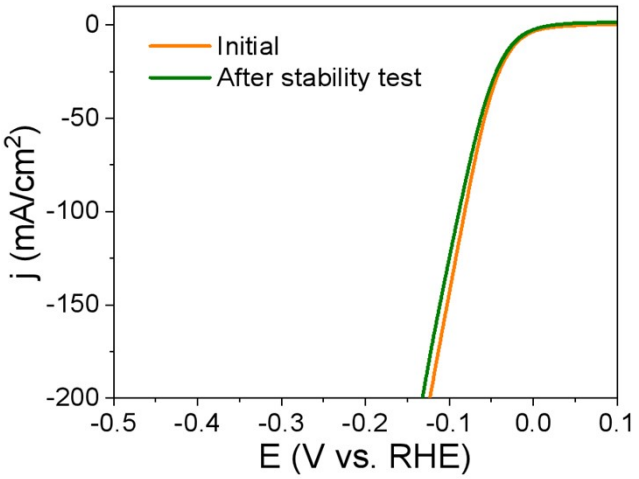

Fig. S7. LSV curves after long-term stability.

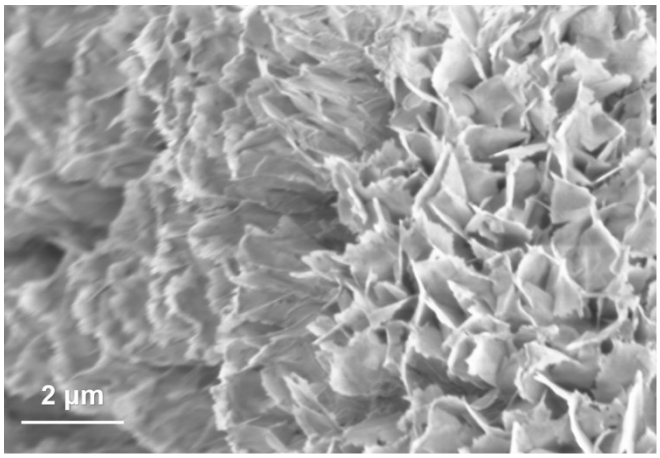

Fig. S8. SEM image of Pt/Ni-BPDC after HER stability.

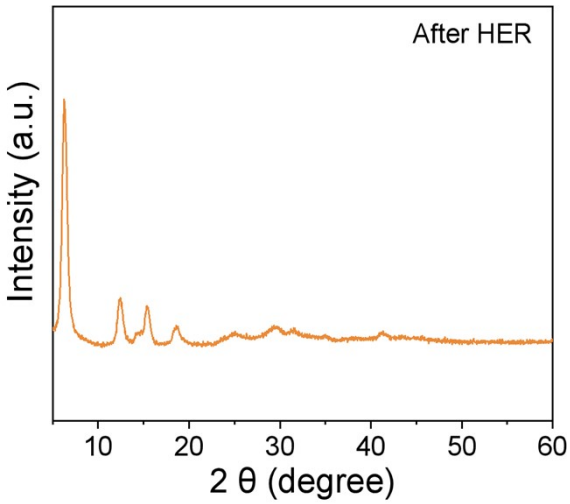

Fig. S9. XRD pattern of Pt/Ni-BPDC after HER stability.

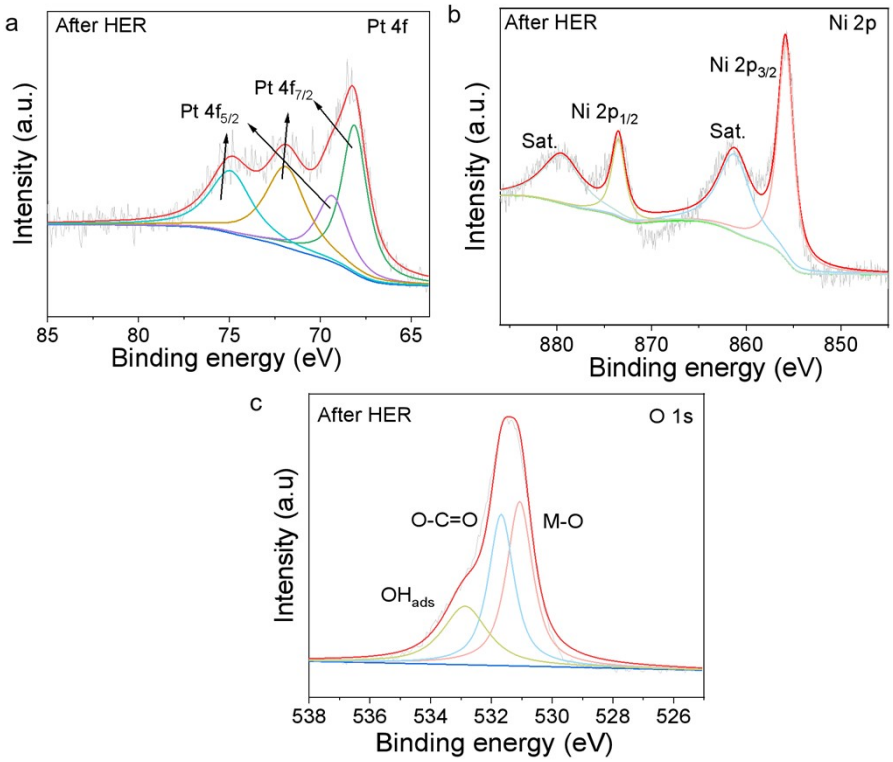

Fig. S10. XPS pattern of Pt/Ni-BPDC after HER stability.

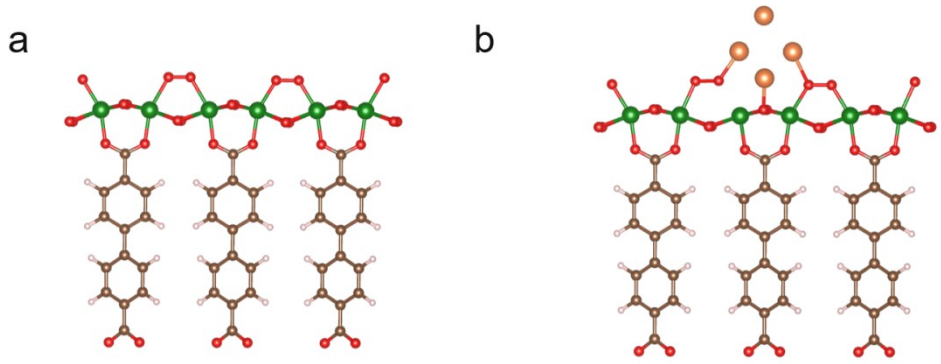

Fig. S11. The optimized (a) Ni-BPDC and (b) Pt/Ni-BPDC models.

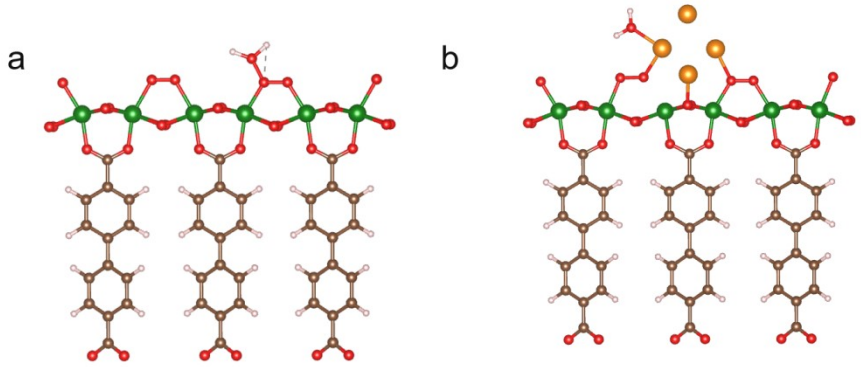

Fig. S12. The optimized model of H_2O on Ni-BPDC and Pt/Ni-BPDC.

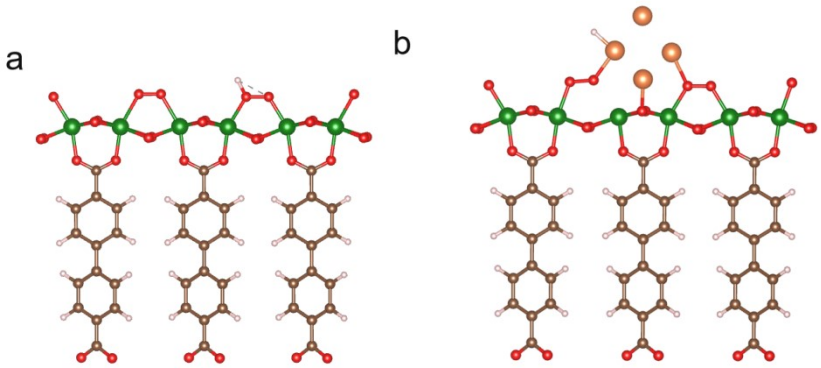

Fig. S13. The optimized model of H on Ni-BPDC and Pt/Ni-BPDC.

Table S1. Comparison of the electrocatalytic performances for HER.

Catalyst	η_{10} (mV)	Tafel slope (mV dec^{-1})	Reference
Pt/Ni-BPDC	25	36.7	This work
Ir/CeO_2	36	33.5	Chem. Comm. 57 (2021), 8798-8801.
Co@Ir/NC-10%	29.4	41.9	ACS. Sustainable Chem.Eng. 2018, 6, 5105-5114.
Ir_1@Co/NC	55	119	Angew. Chem. Inter. Edit. 58 (2019), 11868-11873.
Rh/NiFeRh-LDH	58	81.3	Nano Lett. 2019, 20, 136-144.
CoIr@CN	70	124	J. Mater. Chem. A. 10 (2022), 15543-15553.
IrO_2/V_2O_5	75	48	Adv. Sci. 2022, 9, 2104636.
Ru/MeOH/THF	83	46	Chem. Comm. 53 (2017), 11713-11716.
Ir@NG-750	114	113	J. Mater. Chem. A. 2020, 8, 19665-19673.
Ni-MOF@Pt	102	88	Nano Lett. 19 (2019), 8447-8453.
FeRu-MOF	140	66	J. Mater. Chem. A. 11(2023), 2876-2888.